Pharmacological Research 120 (2017) 242–251

Contents lists available at ScienceDirect

Pharmacological Research

journal homepage: www.elsevier.com/locate/yphrs

Invited Perspective

YM155 induces apoptosis through proteasome-dependent degradation of MCL-1 in primary effusion lymphoma

Yuki Kojima[a], Fumihiko Hayakawa[a,*], Takanobu Morishita[a,b], Keiki Sugimoto[c], Yuka Minamikawa[d], Mizuho Iwase[d], Hideyuki Yamamoto[a], Daiki Hirano[a], Naoto Imoto[a,e], Kazuyuki Shimada[a], Seiji Okada[f], Hitoshi Kiyoi[a]

[a] Department of Hematology and Oncology, Nagoya University Graduate School of Medicine, Nagoya, Japan
[b] Department of Hematology, Japanese Red Cross Nagoya Daiichi Hospital, Nagoya, Japan
[c] Fujii Memorial Research Institute, Otsuka Pharmaceutical Co., Ltd., Otsu, Japan
[d] Department of Analytical Neurobiology, Faculty of Pharmacy, Meijo University, Nagoya, Japan
[e] Department of Hematology, Ogaki Municipal Hospital, Gifu, Japan
[f] Center for AIDS Research, Kumamoto University, Kumamoto, Japan

ARTICLE INFO

Article history:
Received 16 January 2017
Received in revised form 4 April 2017
Accepted 6 April 2017
Available online 8 April 2017

Chemical compounds studied in this article:
YM155 (PubChem CID: 11178236)
U0126 (PubChem CID: 5354033)
Z-VAD-FMK (PubChem CID: 5497174)
Daunorubicin (PubChem CID: 62770)
Idarubicin (PubChem CID: 636362)
Mitoxantrone (PubChem CID: 51082)
6-BIO (PubChem CID: 11405589)
Chicago sky blue 6B (PubChem CID: 9566045)
Pyurvinium pamoate (PubChem CID: 7847555)
Verteporfin (PubChem CID: 5362420)
Licochalcone A (PubChem CID: 5318998)
Tomatine (PubChem CID: 23760126)
Phorbol 12-myristate 13-acetate (PubChem CID: 27924)
Valproic Acid Sodium Salt (PubChem CID: 24277744)

Keywords:
Primary effusion lymphoma
HIV
YM155
Drug screening
Patient-derived xenograft

ABSTRACT

Primary effusion lymphoma (PEL) is a lymphoma that shows malignant effusion in body cavities without contiguous tumor masses and has a very poor prognosis. We recently developed a novel drug screening system using patient-derived xenograft (PDX) cells that maintained the primary cell phenotype better than cell lines. This screening is expected to discover anti-tumor drugs that have been overlooked by conventional screening using cell lines. We herein performed this screening to identify new therapeutic agents for PEL.

We screened 3518 compounds with known pharmaceutical activities based on cytotoxic effects on PDX cells of PEL and selected YM155, a possible survivin inhibitor. It exerted strong anti-tumor effects in PDX cells and three cell lines of PEL; the GI_{50} of YM155 was 1.2–7.9 nM. We found that YM155 reduced myeloid cell leukemia-1 (MCL-1) protein levels prior to decreasing survivin levels, and this was inhibited by a proteasome inhibitor. The knockdown of MCL-1 by siRNA induced cell death in a PEL cell line, suggesting the involvement of decreased MCL-1 levels in YM155-induced cell death. YM155 also induced the phosphorylation of ERK1/2 and MCL-1, and a MEK1 inhibitor inhibited the phosphorylation of ERK1/2, degradation of MCL-1, and YM155-induced apoptosis. These results indicate that YM155 induces the proteasome-dependent degradation of MCL-1 through its phosphorylation by ERK1/2 and causes apoptosis in PEL cells. Furthermore, a treatment with YM155 significantly inhibited the development of ascites in PEL PDX mice. These results suggest the potential of YM155 as an anti-cancer agent for PEL.

1. Introduction

Primary effusion lymphoma (PEL) is a distinct subtype of non-Hodgkin lymphoma (NHL) that most commonly occurs in human immunodeficiency virus-1 (HIV-1)-infected patients, and

* Corresponding author at: Department of Hematology and Oncology Nagoya University, Graduate School of Medicine, 65 Tsurumai-cho, Showa-ku, Nagoya, 466-8550, Japan.
E-mail address: bun-hy@med.nagoya-u.ac.jp (F. Hayakawa).

http://dx.doi.org/10.1016/j.phrs.2017.04.006
1043-6618/

shows malignant effusion in body cavities without contiguous tumor masses [1–3]. Continuous infection by human herpesvirus-8 (HHV-8) due to immunodeficiencies in patients contributes to the oncogenesis of PEL [4,5]. PEL develops rapid resistance to conventional chemotherapy and is an intractable disease with a median survival of 6 months [3,6]. Therefore, there is an urgent need for new therapeutic approaches for PEL; however, the rarity of PEL and lack of suitable animal models have hindered the development of new anti-tumor drugs for this disease.

We previously established a patient-derived xenograft (PDX) model of PEL using a peritoneal inoculation of lymphoma cells derived from a PEL-bearing patient into immunodeficient mice [7]. We also established a cell line from the same primary PEL cells, designated as GTO cells [8]. Using these models, we demonstrated the anti-tumor effects of several non-conventional anti-tumor drugs such as berberine, an anti-CD47 antibody, and chloroquine [7,9,10]; however, we have never attempted high-throughput screening using these models of PEL.

Cell lines are commonly used for high-throughput screening; however, cancer cell lines do not faithfully recapitulate cancer pathology. Microenvironment-independent survival and rapid growth markedly differ between most cell lines and primary tumor cells [11]. It currently remains unclear how these differences affect drug sensitivities. We developed PDX cell screening, in which tumor cells obtained from PDX mice are used for high-throughput screening. We searched for anti-tumor drugs for diffuse large B cell lymphoma (DLBCL) and Philadelphia chromosome-positive acute lymphoblastic leukemia using PDX cell screening [12,13]. We observed marked differences in drug sensitivities between PDX cells and cell lines with the same disease, and identified drugs specifically effective for PDX cells as anti-tumor drugs that had been overlooked by conventional screening using cell lines [13]. However, since the origins of PDX cells and cell lines were different patients, how differences in the nature of PDX cells and cell lines affect drug sensitivities, excluding those due to differences among individuals, remain unknown.

In order to develop novel therapeutic approaches for PEL and clarify the significance of using PDX cells in drug screening, we herein performed high-throughput drug screening using PDX cells and cell lines derived from the same patient with PEL. We revealed that PDX cells were more sensitive to oxidative stress than the cell lines and identified YM155 as a promising anti-tumor drug for PEL.

2. Materials and methods

2.1. Cells and cell culture

The PDX model of PEL (PEL-PDX mice) and GTO cells were established as previously described [7]. Cells obtained from PEL-PDX mice (PEL-PDX cells) and GTO cells were maintained in RPMI supplemented with 20% fetal bovine serum (FBS). BCBL-1 (obtained through the AIDS Research and Reference Reagent Program, Division of AIDS, NIH, Bethesda, MD), BC-1 (purchased from the ATCC, Rockville, MD), and BLS-4 (kindly provided by Dr. Tomoya Katakai, Niigata University, Niigata, Japan) were previously described [4,14,15] and maintained in RPMI supplemented with 10% FBS. None of the cell lines were tested for authentication in our laboratory.

2.2. Reagents and antibodies

YM155 was purchased from Cayman Chemical (Ann Arbor, MI). Z-VAD-FMK was from ENZO Life Sciences (Farmingdale, NY). U0126 was obtained from Promega (Madison, WI). Anti-surivivin, anti-MCL, anti-phospho-MCL-1 (Thr163), anti-cleaved caspase-3, anti-cleaved caspase-7, anti-cleaved PARP, and anti-beta actin antibodies were purchased from Cell Signaling Technology (Beverly, MA).

2.3. Compound library

Among a library of 3518 compounds, 3440 mainly consisting of off-patent drugs and pharmacologically active reagents were kindly provided by the Drug Discovery Initiative (the University of Tokyo, Tokyo, Japan), and 78 compounds consisting of molecular targeting inhibitors were generously provided by the Screening Committee of Anticancer Drugs (Tokyo, Japan).

2.4. PDX cell screening and cell line screening

The methods used for PDX cell screening were previously described [12,13]. Briefly, BLS4 cells (1×10^3/well) were seeded on 96-well plates. On the next day, PEL-PDX cells obtained from sacrificed PEL-PDX mice were seeded (1×10^4/well) and the library compounds (2 μM each) were added to each well. After a 48 h exposure of compounds, total and dead PDX cells were stained with Hoechst 33342 and propidium iodide (PI, Sigma-Aldrich, St Louis, MO), respectively. Total and dead PDX cells were counted separately from BLS4 cells using an Array Scan VTI HCS image analyzer (Thermo Fisher Scientific, Waltham, MA). In the present study, the same method was applied to cell line screening using GTO cells.

2.5. Detection of apoptosis and ROS generation

These assays were performed as described previously, except that a different fluorogenic probe (CellROX Green Reagent, Thermo Fisher Scientific) was used to detect ROS production [12].

2.6. Immunoblot analysis

This was performed as described previously [16]. All immunoblots were performed three times and the intensities of the observed bands were quantified and statistically analyzed by the Student's *t*-test (two-tailed).

2.7. Cell cycle analysis

After washing with PBS, GTO cells were resuspended in PI staining buffer (50 μl/ml PI, 20 μg/ml RNAse, and 0.2% Triton X), incubated at 37° C for 15 min, and analyzed for cell cycle distribution with a flow cytometer (FACSAria, BD Biosciences, San Jose, CA).

2.8. MCL-1 knockdown

MCL-1 siRNA was purchased from Life Technologies and introduced into BCBL-1 cells with nucleofector (Lonza, Wuppertal, Germany) using the program of T-001 and according to the manufacturer's instructions.

2.9. Quantification of viral genes

The expression of viral genes such as *regulator of transcription activation (RTA)* and *latency-associated nuclear antigen (LANA)* was quantified by quantitative RT-PCR as described previously [8], except that the *glyceraldehyde-3-phosphate dehydrogenase (GAPDH)* gene was used as an internal control. Phorbol 12-myristate 13-acetate (PMA: Wako Pure Chemical, Osaka, Japan) was used as an inducer of the lytic replication of HHV-8.

2.10. Animals and estimation of in vivo effects of compounds

Seven-week-old male NOD/SCID IL-2Rγc$^{-/-}$ (NOG) mice (23–25 g) were purchased from In-Vivo Science Inc. (Tokyo, Japan). They were maintained with free access to pellet food and water in plastic cages at 21 ± 2 °C and kept under a 12-h light-12-h dark cycle. PEL-PDX cells (1×10^7/mouse) were injected intraperitoneally into male NOG mice, which were then treated with vehicle or YM155 (5 mg/kg/day) between days 2 and 22. YM155 was administered by continuous subcutaneous infusion using Alzet osmotic pumps (Alzet, Cupertino, CA). All mice were sacrificed by the inhalation of CO_2 on day 22 and the volume of ascites was measured. All animal experiments were approved by the Nagoya University Animal Ethics Committee.

2.11. Statistical analyses

Differences between two groups were analyzed with the Mann-Whitney *U* test and Student's *t*-test (two-tailed). Statistical analyses were performed using SPSS software v23.0 (SPSS Inc., Chicago, IL) and differences with p values less than 0.05 were considered to be significant. Values are presented as the mean ± SEM.

3. Results

3.1. Establishment and characterization of PDX cell screening for PEL

PEL-PDX mice have already been established [7]. PEL-PDX cells were obtained from the ascites of PEL-PDX mice and were positive for markers of PEL cells such as CD38, CD138, and LANA, as reported previously [8]. Their tumor cell ratio measured by the positivity of the human CD45 antigen was 92.9% on average. We established an *ex vivo* culture of PEL-PDX cells. PEL-PDX cells did not survive for a long period of time in the mono-culture, whereas a co-culture with BLS4 cells, which are murine fibroblastic reticular cells, improved survival, as we reported previously using other lymphoma PDX cells [12]. The viability of control PEL-PDX cells was maintained at more than 80% during the entire culture period for PDX cell screening, namely, 48 h, by the co-culture (Fig. 1A).

We then performed drug screening of a library containing 3518 known pharmacologically active substances and off-patent drugs using PEL-PDX cells co-cultured with BLS4 cells, as described previously (PDX cell screening) [12,13]. In order to clarify the characteristics of PDX cell screening and cell line screening (see the Introduction), we performed screening using the cell line, GTO, which we previously established from the same primary cells as those used for the establishment of PEL-PDX cells (GTO screening) [8]. Screening was performed well with Z'-factors of 0.84 and 0.81 and coefficients of variation of 5.31% and 2.50% for PDX cell screening and GTO screening, respectively. All compounds were plotted on scattergrams, on which the viabilities of PDX cells and GTO cells were set on the Y-axis and X-axis, respectively (Fig. 1B). Compounds with viabilities less than 0.5 were discriminated as effective compounds in each screening. PEL-PDX and GTO cells showed similar drug sensitivity profiles to all the compounds tested and the corrrelation coefficient between them was 0.67. This result was attributed to most compounds not exerting anti-tumor effects in either cell. When we focused on compounds that were effective in either cell, PEL-PDX and GTO cells had markedly different drug sensitivity profiles. Only 64 out of 135 effective compounds (47%) in GTO screening were also effective in PDX cell screening. The correlation coefficient between them was −0.07. In order to investigate the characteristics of drugs that were selectively effective in PDX cells, we selected 20 drugs that were at least 2-fold more effective for PDX cells than for GTO cells and designated them as PDX-preferred drugs. The 78 drugs that were at least 2-fold more effective for GTO cells than for PDX cells were named cell line-preferred drugs. PDX-preferred and cell line-preferred drugs were plotted in red and blue, respectively, in Fig. 1B. They were classified into 10 groups by their putative mechanisms of action in the literature (Drug category). Their names, a brief description on their mechanisms of action, and Drug category are summarized in Supplemental Table 1 (PDX-preferred drugs) and Supplemental Table 2 (cell line-preferred drugs). Oxidative stress inducers were frequently detected among PDX-preferred drugs (Fig. 1C), suggesting that PDX cells are sensitive to oxidative stress. Furthermore, reactive oxygen species (ROS) production was the mechanism of action of pyruvinium pamoate and verteporfin, which were the drugs selected in our recent PDX cell screening studies [12,13]. Therefore, we compared ROS production between available PDX-preferred (n = 17) and cell line-preferred (n = 75) drugs. ROS production by PDX-preferred drugs was significantly higher than that by cell line-preferred drugs (Fig. 1D). Median relative ROS production was 0.76 *vs.* 0.26 ($p < 0.001$). These results indicate that PDX cells are sensitive to oxidative stress and also that PDX cell screening is more likely to select drugs that induce ROS production.

3.2. YM155 exerted strong anti-tumor effects on PEL by inducing caspase-dependent apoptosis

The top 10 compounds were selected according to the viability of PDX cells in PDX cell screening. We then measured the viability of cells after the exposure of these compounds at various concentrations more precisely using flow cytometry and calculated the 50% growth-inhibitory concentration (GI_{50}). A list of the top 10 compounds with GI_{50} for PEL-PDX cells and 3 types of PEL cell lines are shown in Table 1. The low viability of cells after the exposure of Chicago sky blue in PDX cell screening was not reproduced by the flow cytometric analysis, and this may have been because the strong color of this compound affected the measurement of viability by the image analyzer in PDX cell screening and caused false positives in the screening. By taking achievable blood concentrations in mice and other factors into consideration, we finally selected YM155, a possible survivin inhibitor, as the best candidate. The structure of YM155 is shown in Fig. 2A. It exerted strong and dose-dependent anti-tumor effects on PEL-PDX cells and all 3 PEL cell lines (Fig. 2A). Its GI_{50} values for the 48-h treatment in PEL-PDX, GTO, BCBL-1, and BC-1 cells were 7.8 nM, 4.3 nM, 7.9 nM, and 1.2 nM, respectively (Table 1).

YM155 has been reported to induce apoptosis by reducing survivin expression levels in several hematological cancer cells [17–19]; therefore, we examined the induction of apoptosis by YM155. An increase in the ratio of apoptotic cells without significant cell cycle arrest was observed in YM155-treated GTO cells (Fig. 2C). This apoptosis was inhibited by the pan-caspase inhibitor, Z-VAD-FMK (Fig. 2D). Consistent with this result, Z-VAD-FMK inhibited the YM155-induced cleavage of caspase-3, caspase-7, and PARP (Fig. 2E). Furthermore, the expression level of myeloid cell leukemia-1 (MCL-1), an anti-apoptotic BCL2-family protein, was reduced by the YM155 treatment; however, the expression level of survivin was not significantly affected (Fig. 2E). YM155-induced PARP activation and reductions in MCL-1 with the intact expression of survivin were also observed in 2 other PEL cell lines (Supplemental Fig. 1A and B). These results indicate that YM155 induces caspase-dependent apoptosis in PEL cells and also that decreased MCL-1 levels are a trigger for caspase activation.

We tested whether YM155 enhanced the lytic or latent replication of HHV-8 by quantifying viral genes such as *RTA* and *LANA* using

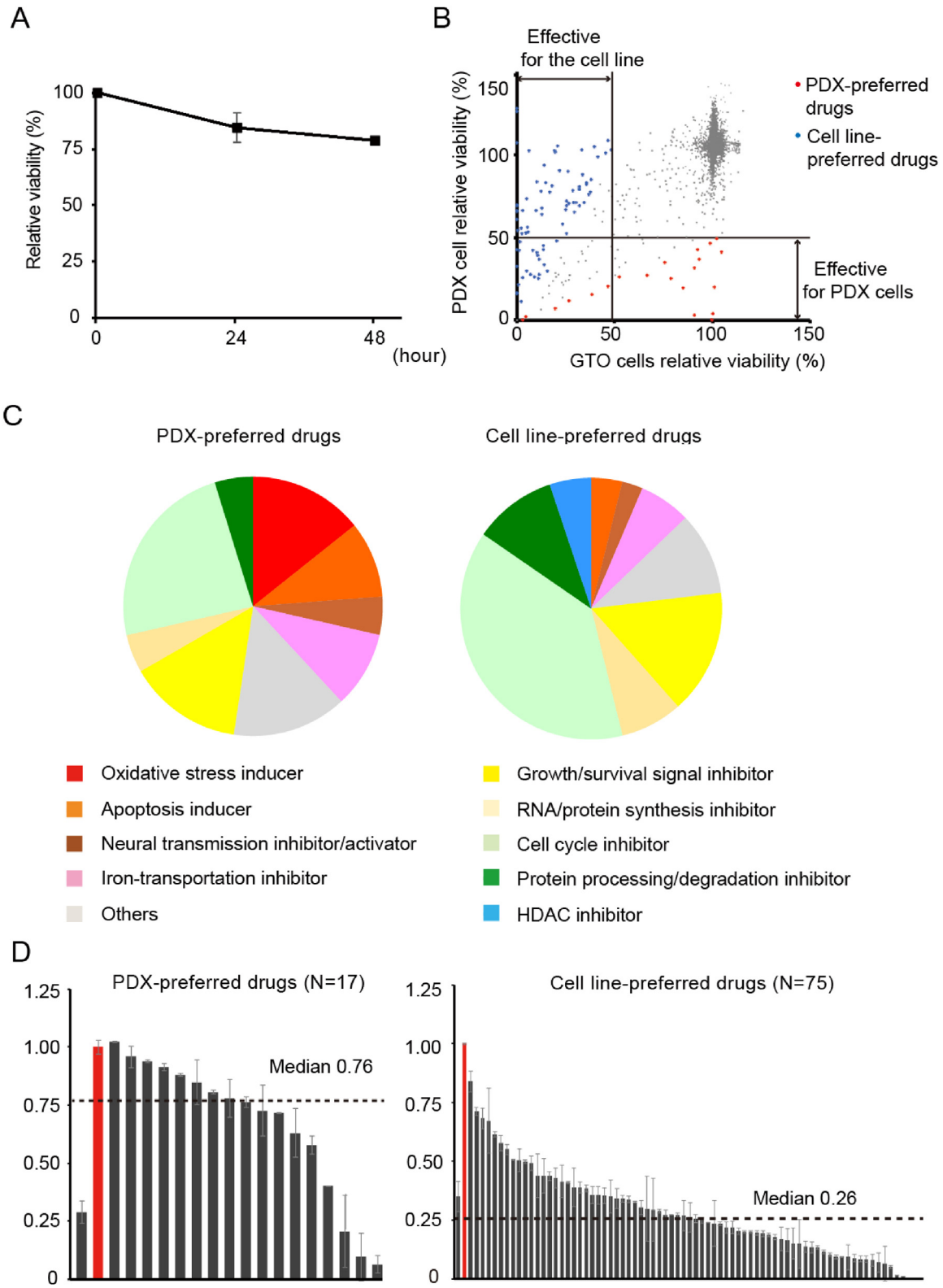

Fig. 1. Establishment and characterization of PDX cell screening for PEL. (A) *Ex vivo* survival of PEL-PDX cells in a co-culture with fibroblastic reticular cells. PEL-PDX cells were cultured with BLS4 cells. Viability was measured using the trypan blue exclusion method. (B) Comparison of drug sensitivity profiles between PDX cells and a cell line. We performed PDX cell screening and GTO screening using a library of 3518 compounds. All compounds were plotted on a scattergram, on which the relative viabilities of PDX and GTO cells were set on the Y-axis and X-axis, respectively. Relative viabilities are relative values to those of control cells treated with vehicle (DMSO). Compounds plotted under the horizontal line or left to the vertical line were judged to be effective drugs for PDX or GTO cells, respectively. PDX-preferred and cell line-preferred drugs are plotted in red and blue, respectively. (C) Comparison of drug classification between PDX-preferred and cell line-preferred drugs. (D) ROS production in PDX cells treated with PDX-preferred and cell line-preferred drugs. PEL-PDX cells were incubated with PDX-preferred and cell line-preferred drugs (2 μM) or menadione (50 μM) for 3 h. ROS production was measured by CellROX Green Oxidative Stress Reagents and plotted on bar charts as relative values to ROS production by menadione (plotted in red).

Table 1
Top 10 compounds in screening and GI50 of compounds in PEL-PDX and PEL cell lines.

Drug name	Mechanism of anti-cancer	GI_{50} (μM)			
		PEL-PDX	GTO	BCBL-1	BC-1
Idarubicine	Anthracycline	0.008	0.0045	0.0076	0.0051
YM-155	Survivin inhibitor	0.0078	0.0043	0.0079	0.0012
6-BIO	GSK-3/STAT3/PDK1 inhibitor	1.2835	4.7653	4.3003	0.7275
Chicago sky blue 6B	Glutamate transporter inhibit	>100	>100	>100	>100
Pyurvinium pamoate	Oxidative stress inducer	1.8637	1.6147	3.6924	0.4553
Verteporfin	Oxidative stress inducer	2.8679	19.704	10.9172	5.1509
Daunorubicine	Anthracycline	0.0253	0.0256	0.0226	0.0106
Licochalcone A	Oxidative stress inducer	2.3034	5.3333	2.2889	1.987
Tomatine	NFkB/JNK inhibitor	1.8731	1.7506	0.202	0.1926
Mitoxantrone	Anthracycline	0.0058	0.0021	0.2588	0.0019

GSK: glycogen synthase kinase; STAT: signal transducers and activator of transcription; PDK: 3-phosphoinositide dependent protein kinase; NFkB: nuclear factor-kappa B; JNK: c-jun N-terminal kinase.

quantitative PCR. YM155 did not significantly affect the expression of these genes (Supplemental Fig. 2A and B).

3.3. YM155 reduced MCL-1 expression, which led to cell death in PEL cells

Although YM155 was identified as a survivin inhibitor by the screening of survivin promoter inhibitors [20], we observed decreases in MCL-1 levels without reductions in survivin levels (Fig. 2E); therefore, we confirmed the effects of YM155 on the expression of both proteins in time-course and dose-dependent experiments. YM155 reduced MCL-1 protein levels from 12 h after its addition (Fig. 3A) and at a concentration of 10 nM (Fig. 3B), whereas survivin expression levels were not significantly affected under either condition.

We investigated whether decreases in MCL-1 levels affected the survival of PEL cells. BCBL-1 cells were introduced with control or MCL-1 siRNA. The successful knockdown of MCL-1 24 h after siRNA introduction was confirmed by immunoblotting (Fig. 3C). Cell death occurred at a significantly higher rate in cells with the knockdown of MCL-1 at 48 h. The cleavage of PARP was also observed in control cells at 24 h (Fig. 3C). This may have been due to electrical damage caused by nucleofection for the introduction of siRNA. These results suggested that decreases in MCL-1 levels reduced the survival ability of PEL cells and were responsible for YM155-induced cell death.

3.4. YM155 induced the proteasome-dependent degradation of MCL-1 through its phosphorylation by ERK1/2

The effects of MG132, a 26S proteasome inhibitor, on the YM155-induced down-regulation of MCL-1 were examined in order to reveal its mechanism of action. MG132 canceled YM155-induced reductions in MCL-1 levels (Fig. 4A). In addition, MCL-1 with slow migration in electrophoresis, which appeared to be ubiquitinated MCL-1, was detected following the co-treatment with YM155 and MG132 in long exposed images (data not shown). These results suggest that YM155 triggers the ubiquitination and proteasome-dependent degradation of MCL-1.

We then investigated the effects of YM155 on the phosphorylation status of signal transduction components such as STAT 3, AKT, NF-kB, and ERK1/2, and found that ERK1/2 phosphorylation was induced by the YM155 treatment (data not shown). A previous study reported that MCL-1 was phosphorylated by ERK1/2 at threonine 163 and that this phosphorylation functioned for both its degradation and stabilization depending on the combination with its phosphorylation by other kinases [21]; therefore, we examined the effects of ERK1/2 phosphorylation by the YM155 treatment on the phosphorylation and degradation of MCL-1 and YM155-induced apoptosis. The YM155 treatment induced the phosphorylation of ERK1/2 and degradation of MCL-1, which were inhibited by U0126, a specific inhibitor of MEK1 (Fig. 4B). Although YM155-induced MCL-1 phosphorylation was not detected due to reductions in MCL-1 expression levels by degradation (Fig. 4B), MCL-1 phosphorylation was transiently detected prior to its degradation (Fig. 4C). Furthermore, U0126 inhibited the YM155-induced degradation of MCL-1 (Fig. 4B) and apoptosis in GTO cells (Fig. 4D). These results indicate that YM155 induced the degradation of MCL-1 through its phosphorylation at Thr163 by ERK1/2, which led to apoptosis in PEL cells.

3.5. YM155 exerted strong anti-tumor effects on PEL in vivo

In order to assess the *in vivo* effects of YM155, PEL-PDX mice were prepared by a peritoneal inoculation of PEL-PDX cells (1×10^7 cells/mouse) into NOG mice and then treated with vehicle or YM155 (5 mg/kg) from days 2–22. YM155 was administered by a continuous subcutaneous injection using osmotic pumps. PEL-PDX mice developed ascites within 3 weeks after the inoculation (Fig. 5A). The volume of ascites was significantly less in YM155-treated mice than in control mice on day 22 (0.75 ml [median, range 0–2.56 ml] *vs.* 3.96 ml [median, range 0.7–5.29 ml], $p < 0.01$, Fig. 5B). In addition, body weight gains until day 22, mainly due to ascites and tumor growth, were significantly less in YM155-treated mice than in control mice (2.1 g [median, range 0–4.9 g] *vs.* 4.5 g [median, range 0.6–7.3 g], $p < 0.05$, Fig. 5C). No mice in either group died until day 22. These results indicate the strong *in vivo* anti-tumor effects of YM155 on PEL.

4. Discussion

Using PDX cell screening, we herein demonstrated that YM155 exerted strong anti-tumor effects on PEL. It induced the degradation of MCL-1 through MCL-1 phosphorylation by ERK1/2, which led to the induction of apoptosis. YM155 was originally identified as a survivin inhibitor, the activity of which was first characterized by the suppression of survivin promoter activity [20]. Although YM155-induced reductions in survivin levels were confirmed, recent studies demonstrated that decreases in MCL-1 levels were induced by YM155 prior to those in survivin levels and were more responsible for YM155-induced cell death [19,22]. We also confirmed these findings in the present study using PEL cell lines and further clarified that the mechanism of action of YM155-induced decreases in MCL-1 levels was degradation through ERK-induced MCL-1 phosphorylation (Fig. 4A–C). YM155-induced ERK1/2 phosphorylation and its involvement in apoptosis in PEL cells are novel

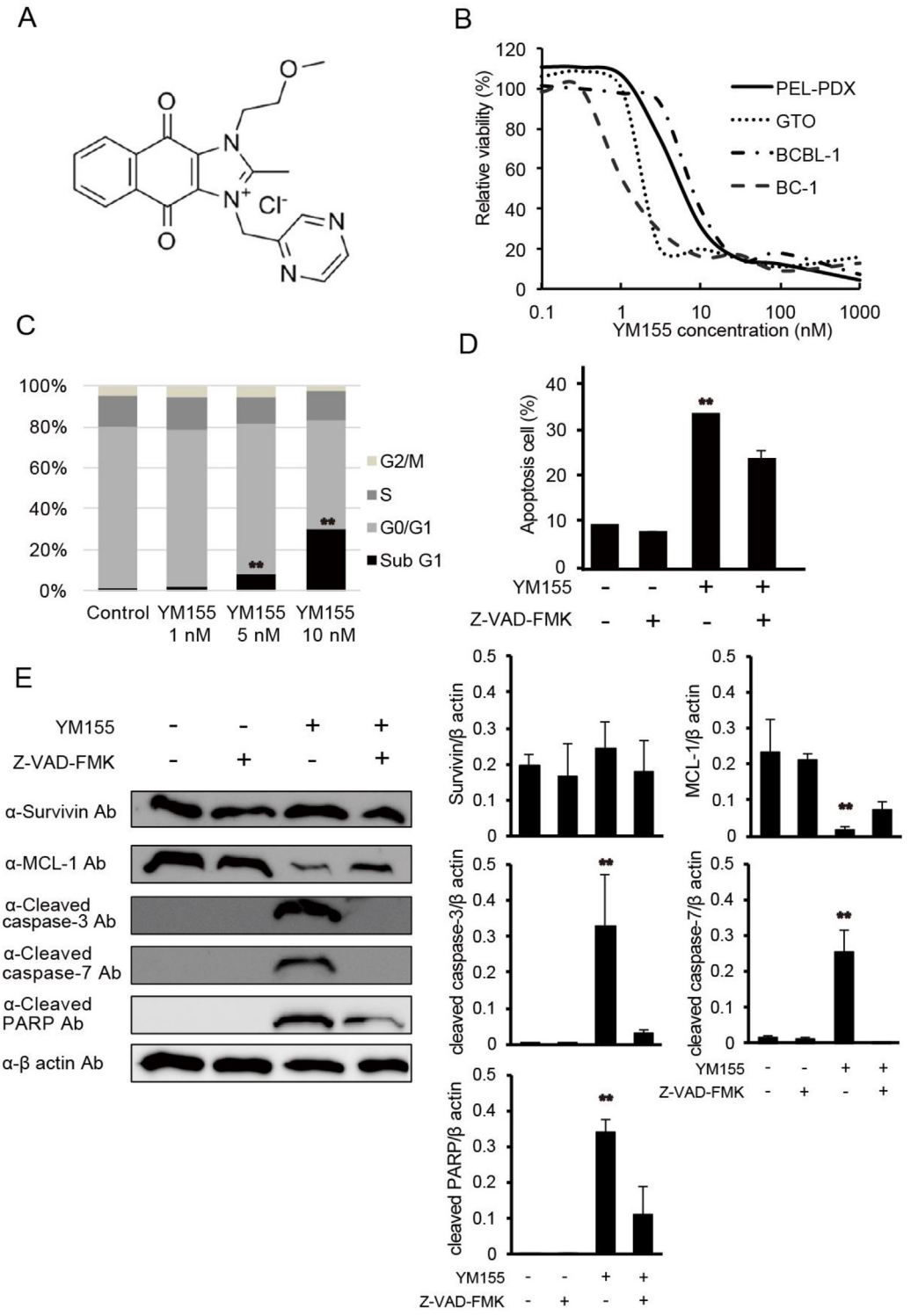

Fig. 2. YM155 exerted strong anti-tumor effects on PEL by inducing caspase-dependent apoptosis (A) Chemical structure of YM155. (B) Dose-response curve of YM155. PEL-PDX cells and 3 PEL cell lines were treated with YM155 at the indicated doses for 48 h. Cell viabilities were measured using a flow cytometer after DAPI staining. (C) Cell cycle analysis of YM155-treated cells. GTO cells were treated with the indicated concentrations of YM155 and stained with PI for a cell cycle analysis after 12 h. Increases in Sub G1 cells were statistically examined. (D) Z-VAD-FMK inhibited YM155-induced apoptosis. GTO cells were treated with YM155 (10 nM) and Z-VAD-FMK (50 μM) as indicated for 24 h. Apoptosis was measured by staining with Annexin-V and PI. (E) YM155 induced the activation of caspase. GTO cells were treated as in (D). Cells were lysed and subjected to immunoblotting with the indicated antibodies. The intensities of the observed bands were quantified and plotted on the bar charts as the mean values of three independent experiments. Error bars indicate the standard deviation. **: $p < 0.01$.

and interesting mechanisms of action because the ERK pathway is more frequently involved in cell survival and proliferation [23]. ERK1/2 activation has also been reported to mediate certain apoptotic signals, such as those induced by the Fas ligand in human neuroblastoma cells, or by transforming growth factor beta (TGFß) in breast carcinoma cells [24,25]. We previously demonstrated that arsenic trioxide-induced apoptosis was mediated through PML phosphorylation by ERK1/2 [16]. MCL-1 phosphorylation at Thr163

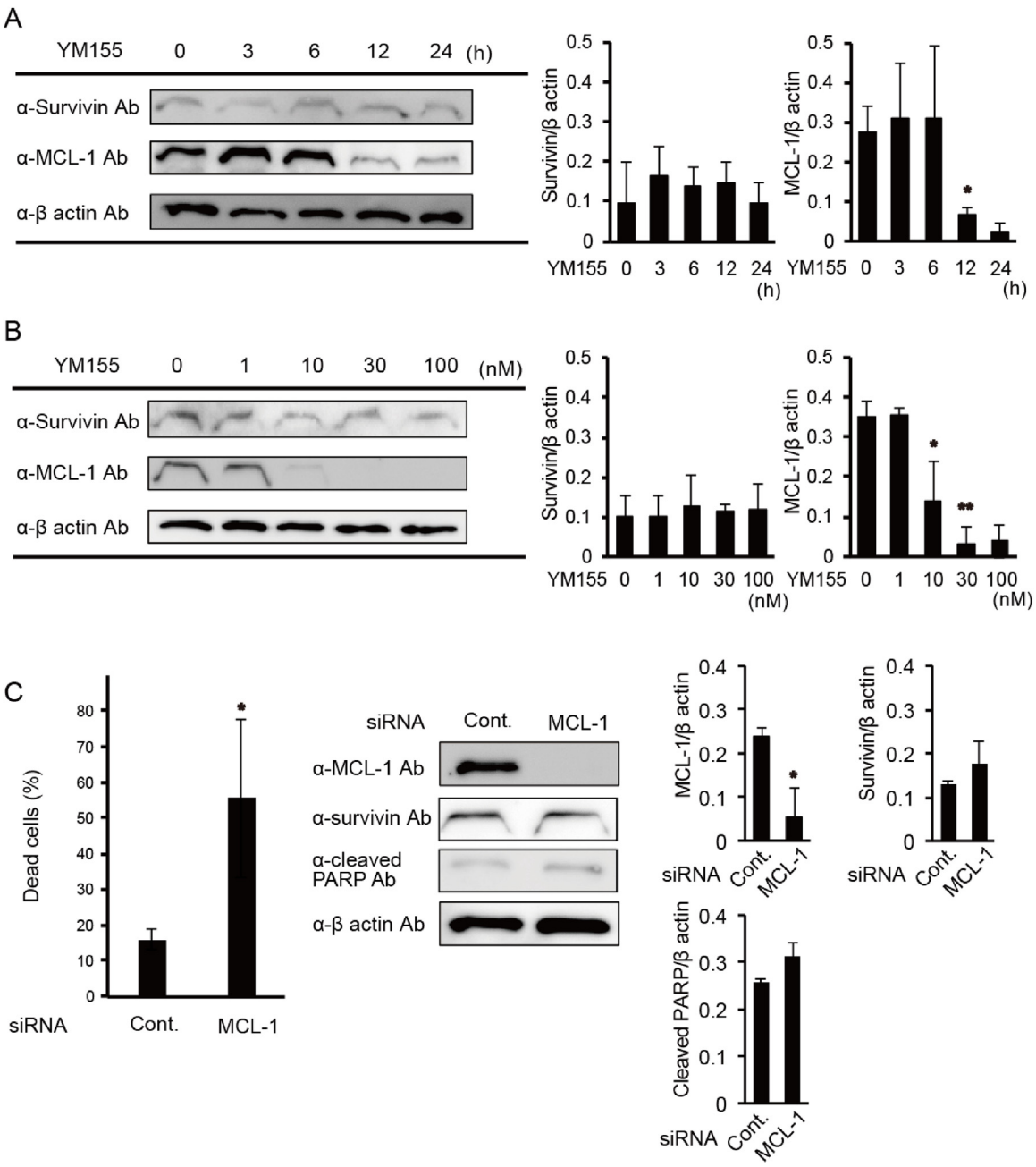

Fig. 3. YM155 reduced MCL-1 expression, which led to cell death in PEL cells. (A) Time-course experiment on decreases in MCL-1 levels by YM155. GTO cells were treated with 10 nM YM155 for the indicated time. Cells were then subjected to immunoblotting, as shown in Fig. 2E. (B) Dose-dependent experiment on decreases in MCL-1 levels by YM155. GTO cells were treated with YM155 at the indicated concentration for 24 h, and analyzed as in (A). (C) The knockdown of MCL-1 induced cell death in PEL cells. Control siRNA (Cont.) or siRNA against MCL-1 (MCL-1) were introduced into BCBL-1 cells by nucleofection. Half of the cells were lysed for immunoblotting after 24 h and the rest were subjected to the measurement of cell death after 48 h. Immunoblotting and the measurement of cell death were performed as shown in Figs. 2E and 2B, respectively. The dead cell ratio was plotted on a bar chart. Each value represents the mean value of three independent experiments performed in triplicate. **: $p < 0.01$, *: $p < 0.05$.

was previously found to initiate phosphorylation at other sites such as Ser155 and Ser159, which led to the degradation of MCL-1 [26]. In the present study, U0126, a highly specific inhibitor of the ERK1/2 pathway, clearly inhibited ERK1/2 phosphorylation, MCL-1 degradation, and YM155-induced apoptosis (Fig. 4B and D), indicating the strong contribution of the ERK1/2 pathway to YM155-induced apoptosis.

Several clinical trials on YM155 for various malignancies, mainly solid tumors, have been performed [27]. Regarding hematological malignancies, a phase I study including 5 patients with NHL and a phase II study for refractory DLBCL (n = 41) have been conducted. In these studies, YM155 showed acceptable toxicity and was tolerated well. Overall response rates were 60% (for 5 NHL) and 7.3%, respectively. The larger study showed limited efficacy; however, DLBCL is a disease entity with a heterogenous genetic background. Therefore, clinical trials on YM155 need to select specific disease subtypes, the survival of which depends on MCL-1 or survivin. PEL is regarded as a genetically homogenous subtype of lymphoma developed by continuous HHV-8 infection. We herein demonstrated the common high efficacy of YM155 among the 3 cell lines tested and PDX cells of PEL, implying the potential of YM155 as a drug for this intractable disease.

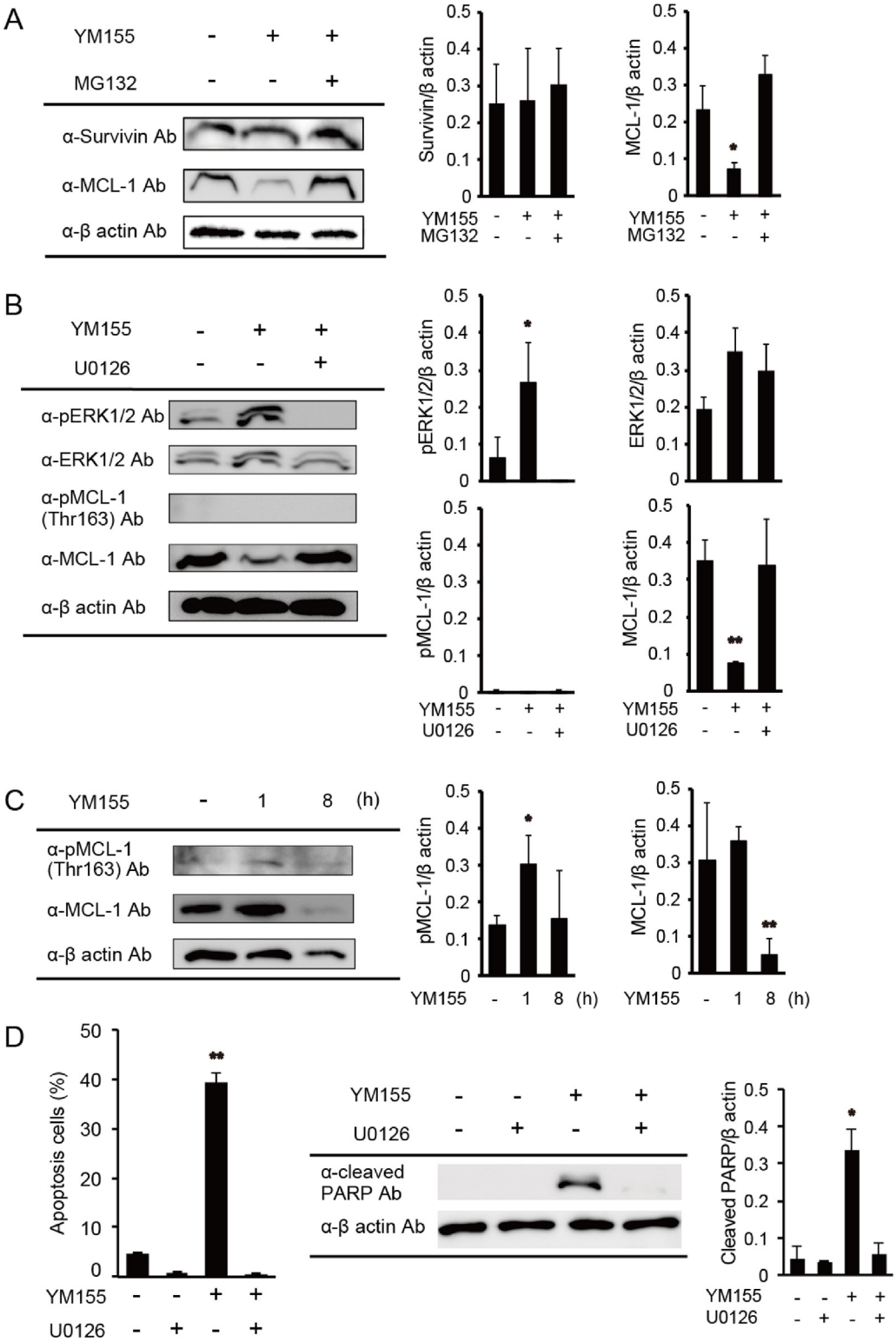

Fig. 4. YM155 induced the proteasome-dependent degradation of MCL-1 through its phosphorylation by ERK1/2. (A) Inhibition of YM155-induced decreases in MCL-1 levels by a proteasome inhibitor. GTO cells were treated with YM155 (10 nM) and MG132 (20 μM) as indicated for 12 h, and subjected to immunoblotting as in Fig. 2E. (B) YM155-induced ERK1/2 phosphorylation and inhibition of the degradation of MCL-1 by a MEK1 inhibitor. GTO cells were treated with YM155 (10 nM) and U0126 (20 μM) as indicated for 8 h, and subjected to immunoblotting as shown in Fig. 2E. (C) YM155-induced phosphorylation of MCL-1. GTO cells were treated with YM155 (10 nM) for the indicated time, and subjected to immunoblotting as shown in Fig. 2E. (D) YM155-induced apoptosis was inhibited by a MEK1 inhibitor. GTO cells were treated with YM155 (10 nM) and U0126 (20 μM) as indicated for 24 h. Apoptosis was measured and presented as in Fig. 2D. **: $p < 0.01$, *: $p < 0.05$.

We clarified that high sensitivity to ROS was a specific characteristic of PDX cells over cell lines (Fig. 1C). Cell lines are often established in culture media containing reducing agents such as 2-mercaptoethanol, which becomes unnecessary after their establishment, suggesting that cell lines develop resistance to oxidative stress during their establishment. ROS production may be a mech-

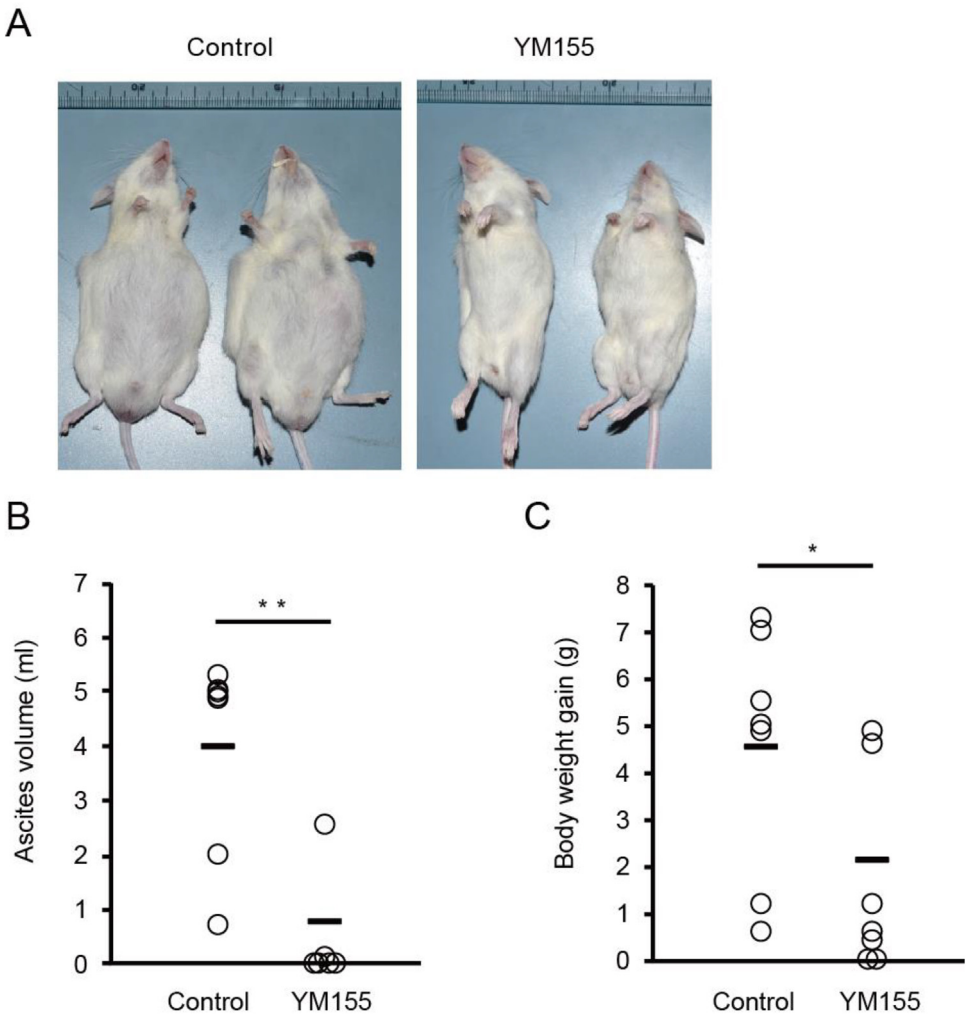

Fig. 5. Anti-tumor effects of YM155 *in vivo*. NOG mice were intraperitoneally inoculated with PEL-PDX cells and treated with 1% DMSO (Control, n = 7) or YM155 (YM155, n = 7) (A) Photographs of mice on day 22. (B) The volume of ascites. All mice were sacrificed on day 22 and the volume of ascites was measured and plotted. (C) Body weight gains. Body weights were measured on days 1 and 22. Body weight gains were plotted. **: $p < 0.01$, *: $p < 0.05$. The horizontal line is the mean of the measurements.

anism of action that has been overlooked or underestimated by conventional anti-cancer drug screening systems using cell lines. PDX cell screening is a useful tool for discovering oxidative stress-inducing drugs; however, the mechanism of action of YM155 was not ROS production. ROS production by YM155 at 10 nM was not high, 0.522-fold higher than that by menadione, and the addition of reduced glutathione, a well-known reducing agent, had a negligible impact on the effects of YM155 (data not shown), indicating the weak contribution of ROS production to YM155-induced cell death. This may be because we selected drugs that exert anti-cancer effects against not only PDX cells, but also cell lines in preference of a wide range of anti-cancer effects among PEL.

In summary, we herein performed PDX cell screening using the PDX cells of PEL and identified YM155 as a promising anti-cancer drug against this intractable disease. By introducing the phenotype of primary cancer cells at earlier *in vitro* stages of drug development, PDX cell screening will provide novel insights for drug development.

Author contributions

F.H. and Y.K. designed the research, performed experiments, and wrote the paper. M.T., K.Sugimoto, Y.M., M.I., D.H., H.Y., and N.I. performed experiments. K. Shimada, S.O., and H.K. designed the research.

Disclosure of conflicts of interest

K. Sugimoto is an employee of Otsuka Pharmaceutical Co. Ltd. H.K. received research funding from Chugai Pharmaceutical Co. LTD., Bristol-Myers Squibb, Kyowa-Hakko Kirin Co. LTD., Zenyaku Kogyo Company LTD., Astellas Pharma Inc., Nippon Boehringer Ingelheim GmbH, Celgene Corporation, and Fujifilm Corporation. The other authors have no potential conflicts of interest.

Grant support

This work was supported by MHLW KAKENHI Grant Number H26- Kakushintekigan-Ippan-133 and JSPS KAKENHI Grant Numbers 25293218, 25670449, and 15K09472. This work was also supported by the Program to Disseminate Tenure Tracking System, MEXT, Japan and the Platform for Drug Discovery, Informatics, and Structural Life Science from the Ministry of Education, Culture, Sports, Science and Technology, Japan.

Acknowledgements

We thank the Drug Discovery Initiative and Screening Committee of Anticancer Drugs for providing the chemical library and are thankful to Dr. Tomoya Katakai and the AIDS Research and Reference Reagent Program for providing cell lines. We are very grateful to Yoko Matsuyama and Chika Wakamatsu for their technical assistance. We would thank to Yukie Konishi, Manami Kira, Rie Kojima and Yuko Kojima for secretarial assistance.

Appendix A. Supplementary data

Supplementary data associated with this article can be found, in the online version, at http://dx.doi.org/10.1016/j.phrs.2017.04.006.

References

[1] D.M. Knowles, G. Inghirami, A. Ubriaco, R. Dalla-Favera, Molecular genetic analysis of three AIDS-associated neoplasms of uncertain lineage demonstrates their B-cell derivation and the possible pathogenetic role of the Epstein-Barr virus, Blood 73 (3) (1989) 792–799.
[2] A.E. Walts, I.P. Shintaku, J.W. Said, Diagnosis of malignant lymphoma in effusions from patients with AIDS by gene rearrangement, Am. J. Clin. Pathol. 94 (2) (1990) 170–175.
[3] C. Simonelli, M. Spina, R. Cinelli, R. Talamini, R. Tedeschi, A. Gloghini, E. Vaccher, A. Carbone, U. Tirelli, Clinical features and outcome of primary effusion lymphoma in HIV-infected patients: a single-institution study, J. Clin. Oncol. 21 (21) (2003) 3948–3954.
[4] E. Cesarman, Y. Chang, P.S. Moore, J.W. Said, D.M. Knowles, Kaposi's sarcoma-associated herpesvirus-like DNA sequences in AIDS-related body-cavity-based lymphomas, N. Engl. J. Med. 332 (18) (1995) 1186–1191.
[5] Y. Chang, E. Cesarman, M.S. Pessin, F. Lee, J. Culpepper, D.M. Knowles, P.S. Moore, Identification of herpesvirus-like DNA sequences in AIDS-associated Kaposi's sarcoma, Science 266 (5192) (1994) 1865–1869.
[6] E. Boulanger, L. Gerard, J. Gabarre, J.M. Molina, C. Rapp, J.F. Abino, J. Cadranel, S. Chevret, E. Oksenhendler, Prognostic factors and outcome of human herpesvirus 8-associated primary effusion lymphoma in patients with AIDS, J. Clin. Oncol. 23 (19) (2005) 4372–4380.
[7] H. Goto, Y. Kojima, K. Matsuda, R. Kariya, M. Taura, K. Kuwahara, H. Nagai, H. Katano, S. Okada, Efficacy of anti-CD47 antibody-mediated phagocytosis with macrophages against primary effusion lymphoma, Eur. J. Cancer 50 (10) (2014) 1836–1846.
[8] H. Goto, Y. Kojima, H. Nagai, S. Okada, Establishment of a CD4-positive cell line from an AIDS-related primary effusion lymphoma, Int. J. Hematol. 97 (5) (2013) 624–633.
[9] H. Goto, R. Kariya, M. Shimamoto, E. Kudo, M. Taura, H. Katano, S. Okada, Antitumor effect of berberine against primary effusion lymphoma via inhibition of NF-kappaB pathway, Cancer Sci. 103 (4) (2012) 775–781.
[10] M. Masud Alam, R. Kariya, A. Kawaguchi, K. Matsuda, E. Kudo, S. Okada, Inhibition of autophagy by chloroquine induces apoptosis in primary effusion lymphoma in vitro and in vivo through induction of endoplasmic reticulum stress, Apoptosis 21 (10) (2016) 1191–1201.
[11] S. Kopetz, R. Lemos, G. Powis, The promise of patient-derived xenografts: the best laid plans of mice and men, Clin. Cancer Res. 18 (19) (2012) 5160–5162.
[12] K. Sugimoto, F. Hayakawa, S. Shimada, T. Morishita, K. Shimada, T. Katakai, A. Tomita, H. Kiyoi, T. Naoe, Discovery of a drug targeting microenvironmental support for lymphoma cells by screening using patient-derived xenograft cells, Sci. Rep. 5 (13054) (2015).
[13] T. Morishita, F. Hayakawa, K. Sugimoto, M. Iwase, H. Yamamoto, D. Hirano, Y. Kojima, N. Imoto, T. Naoe, H. Kiyoi, The photosensitizer verteporfin has light-independent anti-leukemic activity for Ph-positive acute lymphoblastic leukemia and synergistically works with dasatinib, Oncotarget 7 (35) (2016) 56241–56252.
[14] T. Katakai, T. Hara, M. Sugai, H. Gonda, A. Shimizu, Lymph node fibroblastic reticular cells construct the stromal reticulum via contact with lymphocytes, J. Exp. Med. 200 (6) (2004) 783–795.
[15] R. Renne, W. Zhong, B. Herndier, M. McGrath, N. Abbey, D. Kedes, D. Ganem, Lytic growth of Kaposi's sarcoma-associated herpesvirus (human herpesvirus 8) in culture, Nat. Med. 2 (3) (1996) 342–346.
[16] F. Hayakawa, M.L. Privalsky, Phosphorylation of PML by mitogen-activated protein kinases plays a key role in arsenic trioxide-mediated apoptosis, Cancer Cell 5 (4) (2004) 389–401.
[17] J.W. Tyner, A.M. Jemal, M. Thayer, B.J. Druker, B.H. Chang, Targeting survivin and p53 in pediatric acute lymphoblastic leukemia, Leukemia 26 (4) (2012) 623–632.
[18] J. Chen, C.A. Pise-Masison, J.H. Shih, J.C. Morris, J.E. Janik, K.C. Conlon, A. Keating, T.A. Waldmann, Markedly additive antitumor activity with the combination of a selective survivin suppressant YM155 and alemtuzumab in adult T-cell leukemia, Blood 121 (11) (2013) 2029–2037.
[19] W. Feng, A. Yoshida, T. Ueda, YM155 induces caspase-8 dependent apoptosis through downregulation of survivin and Mcl-1 in human leukemia cells, Biochem. Biophys. Res. Commun. 435 (1) (2013) 52–57.
[20] T. Nakahara, A. Kita, K. Yamanaka, M. Mori, N. Amino, M. Takeuchi, F. Tominaga, S. Hatakeyama, I. Kinoyama, A. Matsuhisa, M. Kudoh, M. Sasamata, YM155, a novel small-molecule survivin suppressant, induces regression of established human hormone-refractory prostate tumor xenografts, Cancer Res. 67 (17) (2007) 8014–8021.
[21] K. Fernald, M. Kurokawa, Evading apoptosis in cancer, Trends Cell Biol. 23 (12) (2013) 620–633.
[22] H. Tang, H. Shao, C. Yu, J. Hou, Mcl-1 downregulation by YM155 contributes to its synergistic anti-tumor activities with ABT-263, Biochem. Pharmacol. 82 (9) (2011) 1066–1072.
[23] M.H. Cobb, MAP kinase pathways, Prog. Biophys. Mol. Biol. 71 (3–4) (1999) 479–500.
[24] E. Goillot, J. Raingeaud, A. Ranger, R.I. Tepper, R.J. Davis, E. Harlow, I. Sanchez, Mitogen-activated protein kinase-mediated Fas apoptotic signaling pathway, Proc. Natl. Acad. Sci. U. S. A. 94 (7) (1997) 3302–3307.
[25] R.S. Frey, K.M. Mulder, Involvement of extracellular signal-regulated kinase 2 and stress-activated protein kinase/Jun N-terminal kinase activation by transforming growth factor beta in the negative growth control of breast cancer cells, Cancer Res. 57 (4) (1997) 628–633.
[26] C. Morel, S.M. Carlson, F.M. White, R.J. Davis, Mcl-1 integrates the opposing actions of signaling pathways that mediate survival and apoptosis, Mol. Cell. Biol. 29 (14) (2009) 3845–3852.
[27] A. Rauch, D. Hennig, C. Schafer, M. Wirth, C. Marx, T. Heinzel, G. Schneider, O.H. Kramer, Survivin and YM155: how faithful is the liaison? Biochim. Biophys. Acta 1845 (2) (2014) 202–220.